Auxiliary material for

Dynamic Mantle-Transition-Zone Controls on Upper-Plate Tilt

Fabio Crameri[1] **and Carolina Lithgow-Bertelloni**[2]

[1]Centre for Earth Evolution and Dynamics (CEED), University of Oslo, Norway.
[2]Department of Earth Sciences, University College London, United Kingdom.

Tectonophysics, 2017

Contents

S1 Supplementary Movie

The movie shows the time-evolution comparison between (a-c) the $ViscosityJump$ model with a simple UM-LM viscosity jump, (d-f) the $PhaseTransition$ model that additionally includes an UM-LM phase transition, and (g-i) the $Continent$ model that additionally features a continental upper plate. All experiments feature an initial shallow-slab dip of 30° and shown are a graph of slab-tip depth versus upper-plate tilt with a white dot indicating current time (top row), current surface topography (middle row), and current effective viscosity (bottom row). Red lines indicate the automated tracking of the upper-plate tilt.

S2 Supplementary Figures

See figures and corresponding captions below.

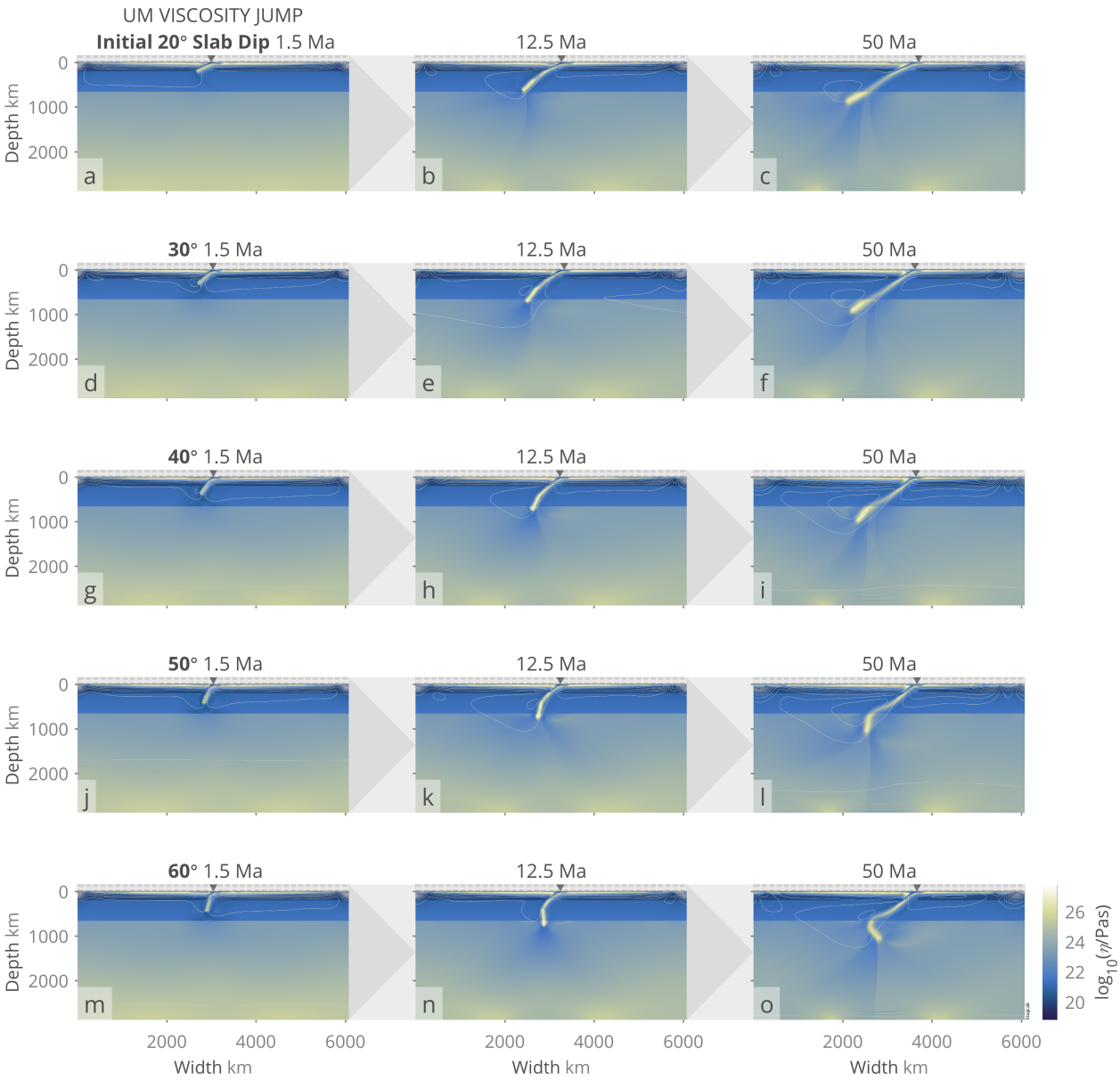

Figure S1: Time evolution (from left to right) of the *ViscosityJump* model with a simple UM-LM viscosity jump for multiple experiments with different initial shallow slab-dip angles ranging from (a-c) 20° to (m-p) 60°. Shown is the effective viscosity and grey lines indicate flow direction.

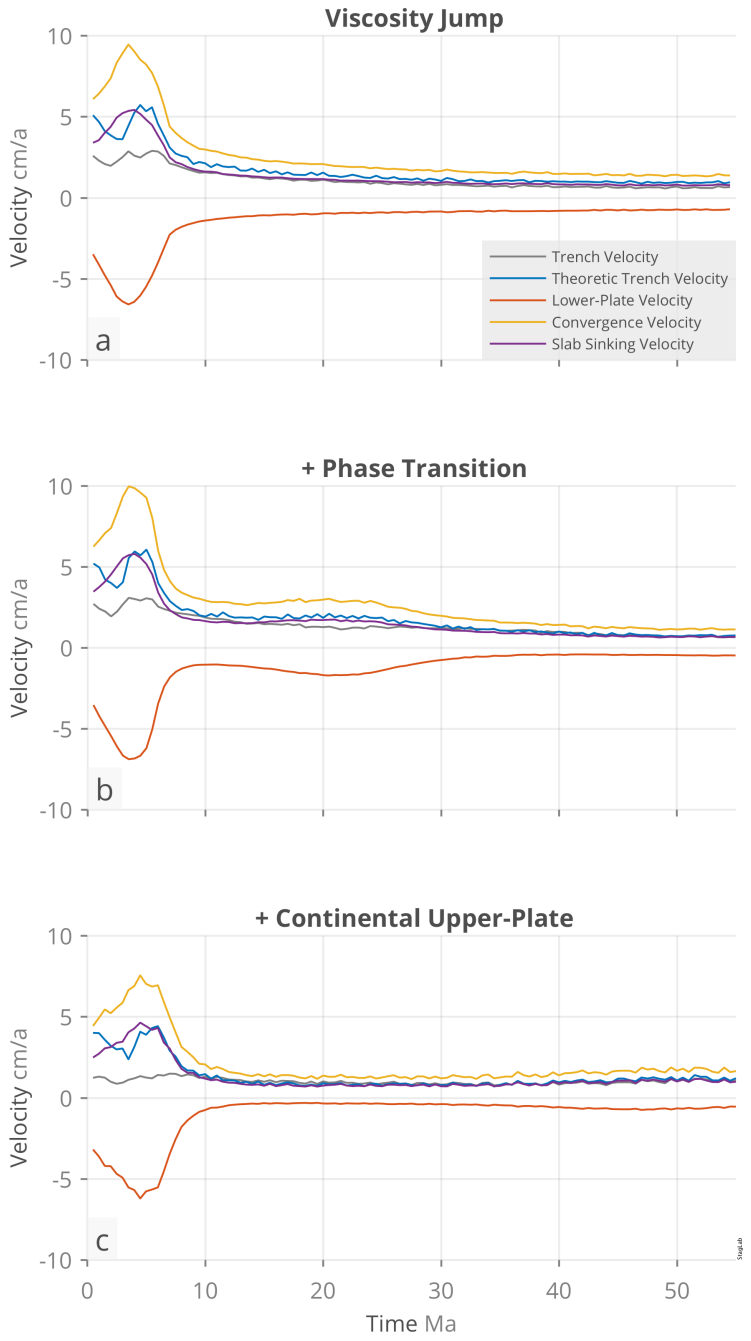

Figure S2: Plate-velocity graph for (a) the *ViscosityJump* model with an UM-LM viscosity jump of factor 100 but no phase transition, (b) the *PhaseTransition* model with an UM-LM viscosity jump of factor 30 and an upper-mantle phase transition, and (c) the *Continent* model with a phase transition and a 2000-km wide continental upper-plate. All models have an initial 30° shallow-slab dip angle. Shown are effective and theoretic trench velocities, lower-plate velocity, slab-sinking velocity, and total plate-convergence velocity.

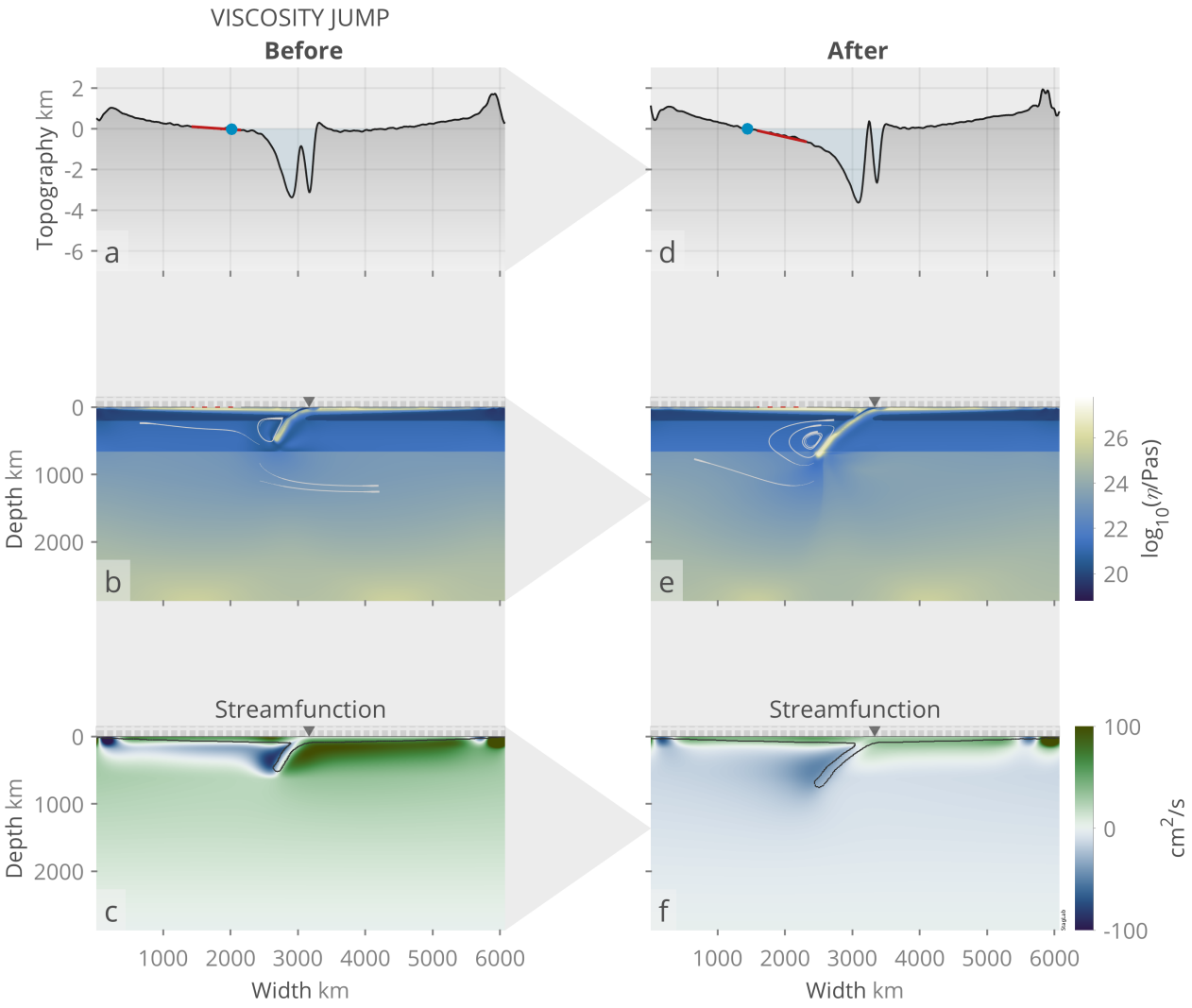

Figure S3: Comparison between (a-c) before and (d-f) after slab-transition zone interaction for the *ViscosityJump* model with a simple UM-LM viscosity jump. Shown are (a,d) surface topography with indicators for upper-plate tilt (red bar) and inundation (blue dot), (b,e) effective viscosity with grey lines indicating flow direction, (c,f) the stream function where blue colours indicate clock-wise direction of the flow and the black contour indicates the position of the plate and slab.

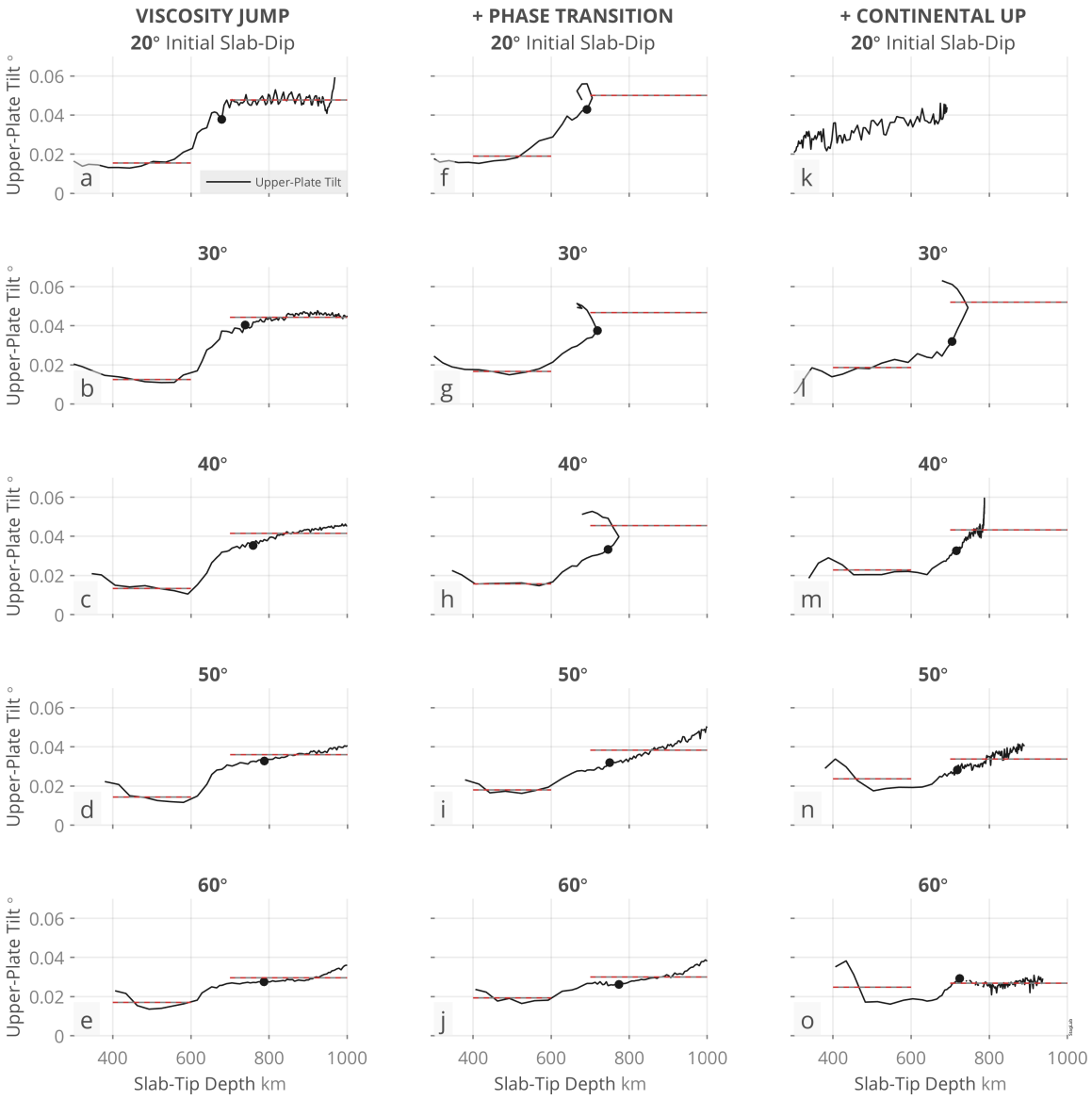

Figure S4: Upper-plate tilt as a function of slab-tip depth shown for (a-e) the *ViscosityJump*, (f-j) the *PhaseTransition*, and (k-o) the *Continent* model setup with variable initial shallow-slab dips ranging between (a,f,k) 20° and (e,j,o) 60°. Black points indicate 12.5 Ma and red-grey dashed lines indicate the mean tilt-values during slab-tip sinking between $400-600$ km depth (i.e., before slab-transition zone interaction) and from the point the slab reaches 700 km depth (i.e., after slab-transition zone collision) to a maximum of 1000 km depth (if reached). The UP-tilt in panel (k) for 20° is strongly biased due to the strong coupling of the shallow slab with the thick continental upper plate (see Section 4 for more details).

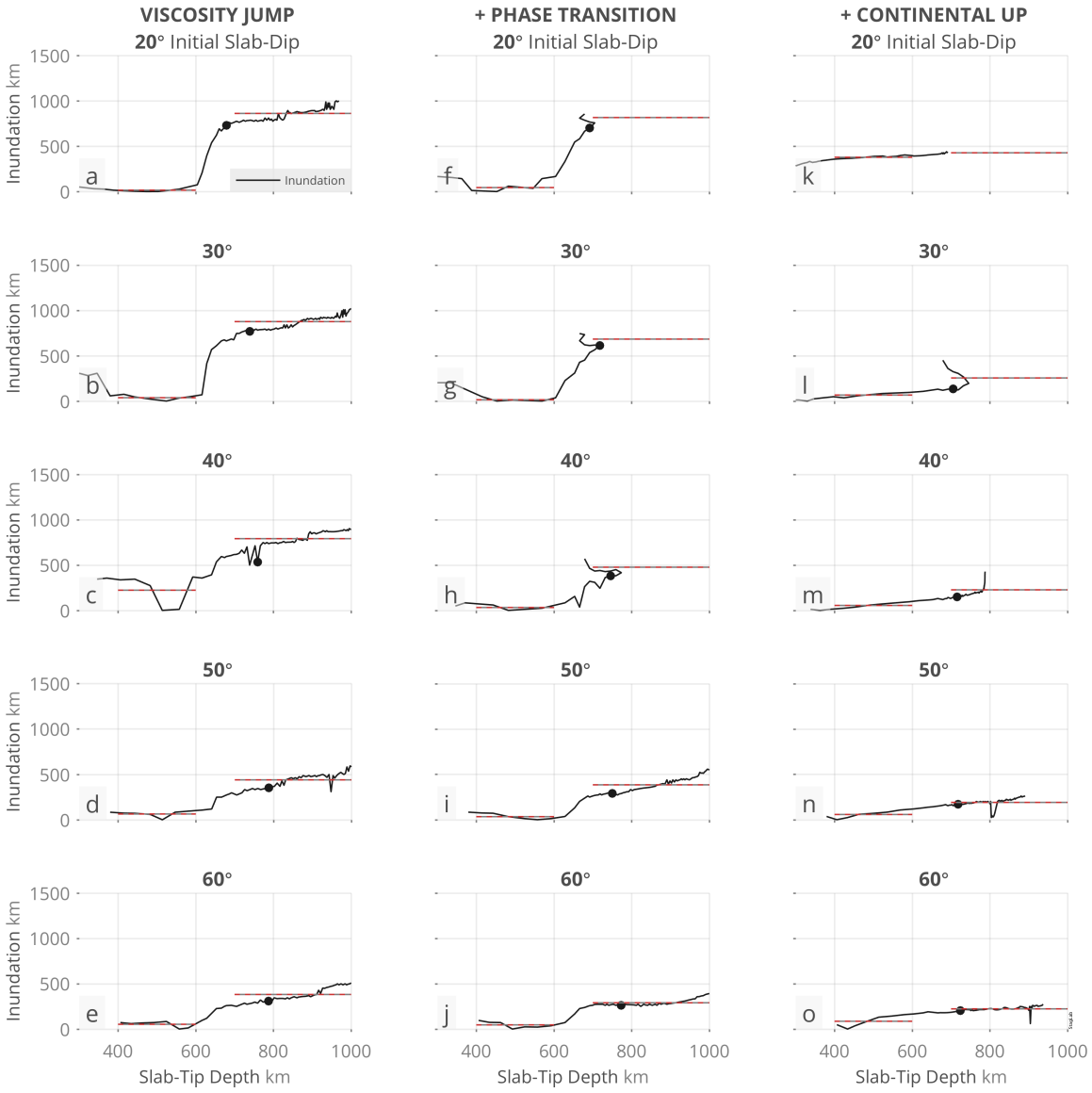

Figure S5: Inundation (normalised to temporal minimum value) as a function of slab-tip depth shown for (a-e) the $ViscosityJump$, (f-j) the $PhaseTransition$, and (k-o) the $Continent$ model setup with variable initial shallow-slab dips ranging between (a,f,k) 20° and (e,j,o) 60°. Black points indicate 12.5 Ma and red-grey dashed lines indicate the mean tilt-values during slab-tip sinking between $400-600$ km depth (i.e., before slab-transition zone interaction) and from the point the slab reaches 700 km depth (i.e., after slab-transition zone collision) to a maximum of 1000 km depth (if reached). The UP-tilt in panel (k) for 20° is strongly biased due to the strong coupling of the shallow slab with the thick continental upper plate (see Section 4 for more details).

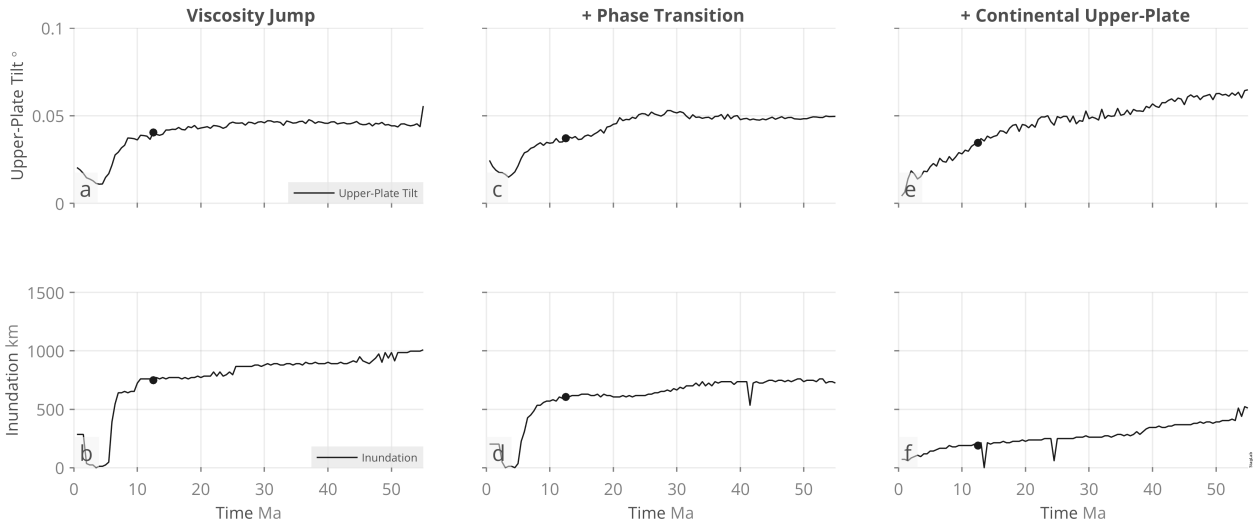

Figure S6: Temporal evolution of absolute upper-plate tilt and variation in artificial inundation during slab-transition zone interaction. Both upper-plate tilt (top row) and artificial inundation (bottom row) are displayed as a function of time and shown for (a,b) the $ViscosityJump$ model with a simple UM-LM viscosity jump, (c,d) the $PhaseTransition$ model that additionally includes an UM-LM phase transition, and (e,f) the $Continent$ model that additionally features a continental upper plate. Black points indicate 12.5 Ma and spikes are caused by rough surface portions that act as a dam that can be suddenly flooded or inhibit further inundation.

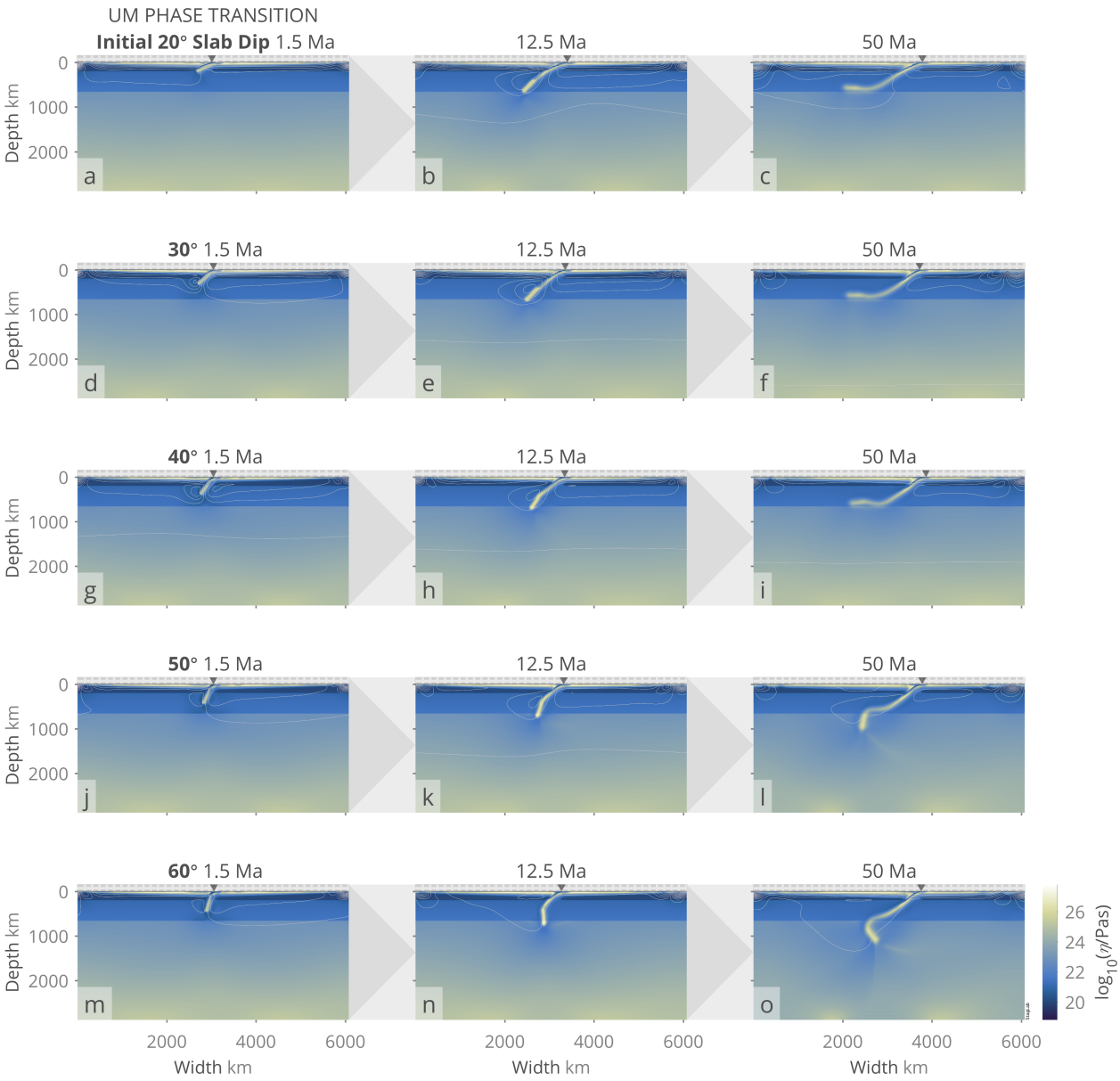

Figure S7: Time evolution (from left to right) of the *PhaseTransition* model for multiple experiments with different initial shallow-slab dip angles ranging from (a-c) 20° to (m-o) 60°. Shown is the effective viscosity and grey lines indicate flow direction.

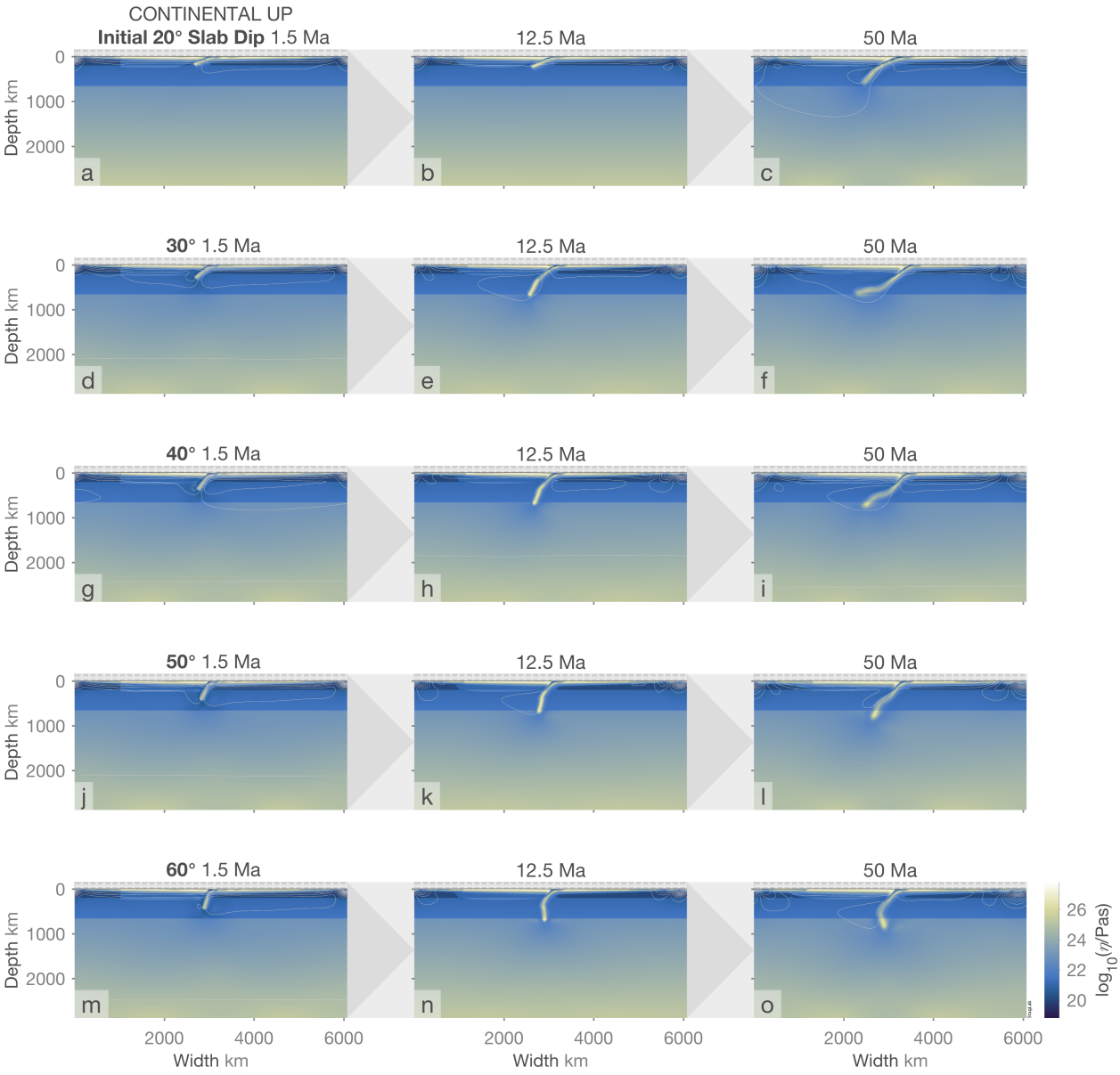

Figure S8: Time evolution (from left to right) of the *Continent* model with a 250-km thick and 2000-km wide continent for multiple experiments employing different initial shallow-slab dip angles ranging from 20° (top row) to 60° (bottom row). Shown is the viscosity and grey lines indicate flow direction.

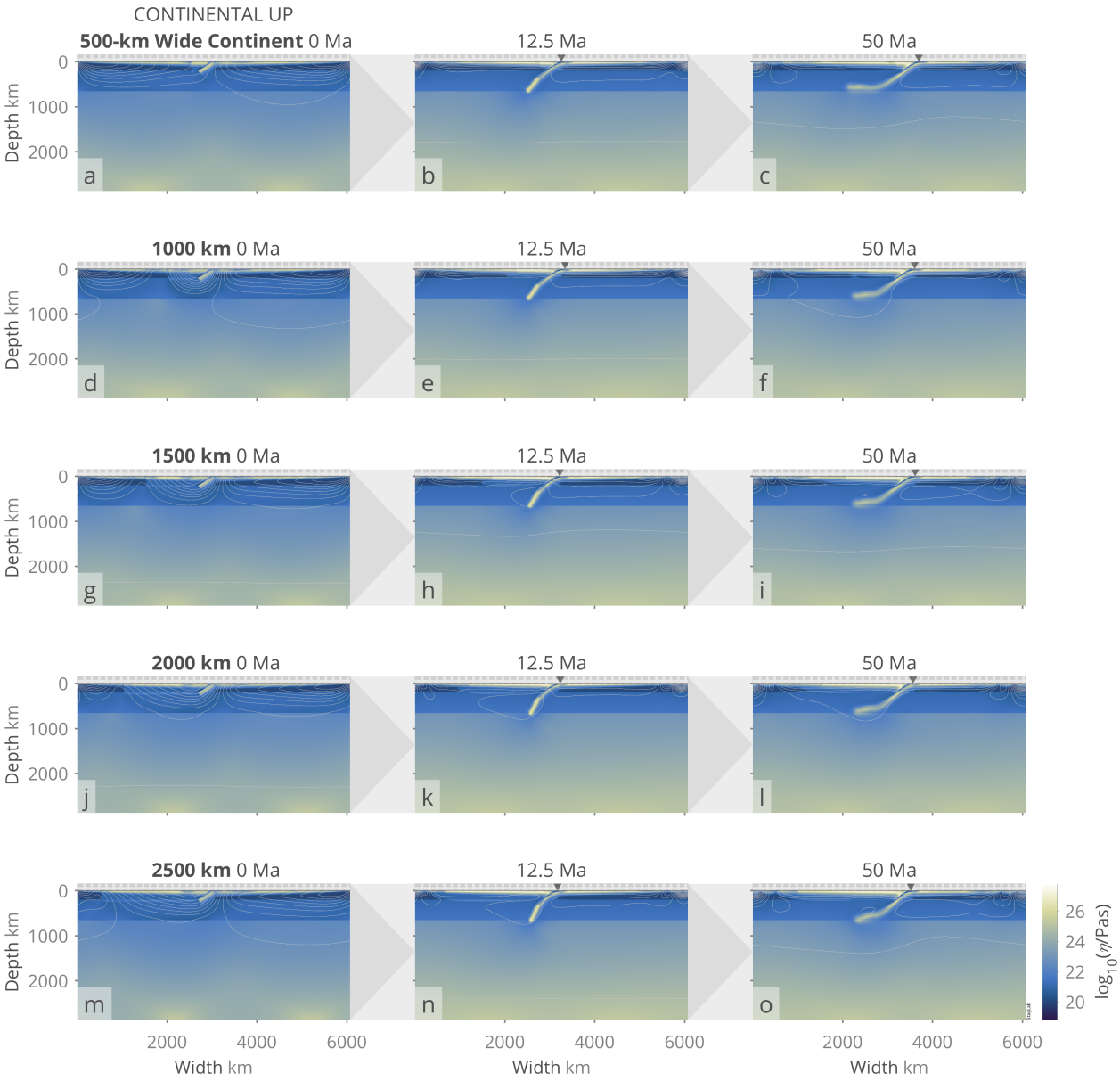

Figure S9: Time evolution (from left to right) for multiple experiments of the *Continent* model employing a 250-km thick and differently-wide continental upper plates ranging from 500 km (top row) to 2500 km (bottom row). Shown is the viscosity and grey lines indicate flow direction.

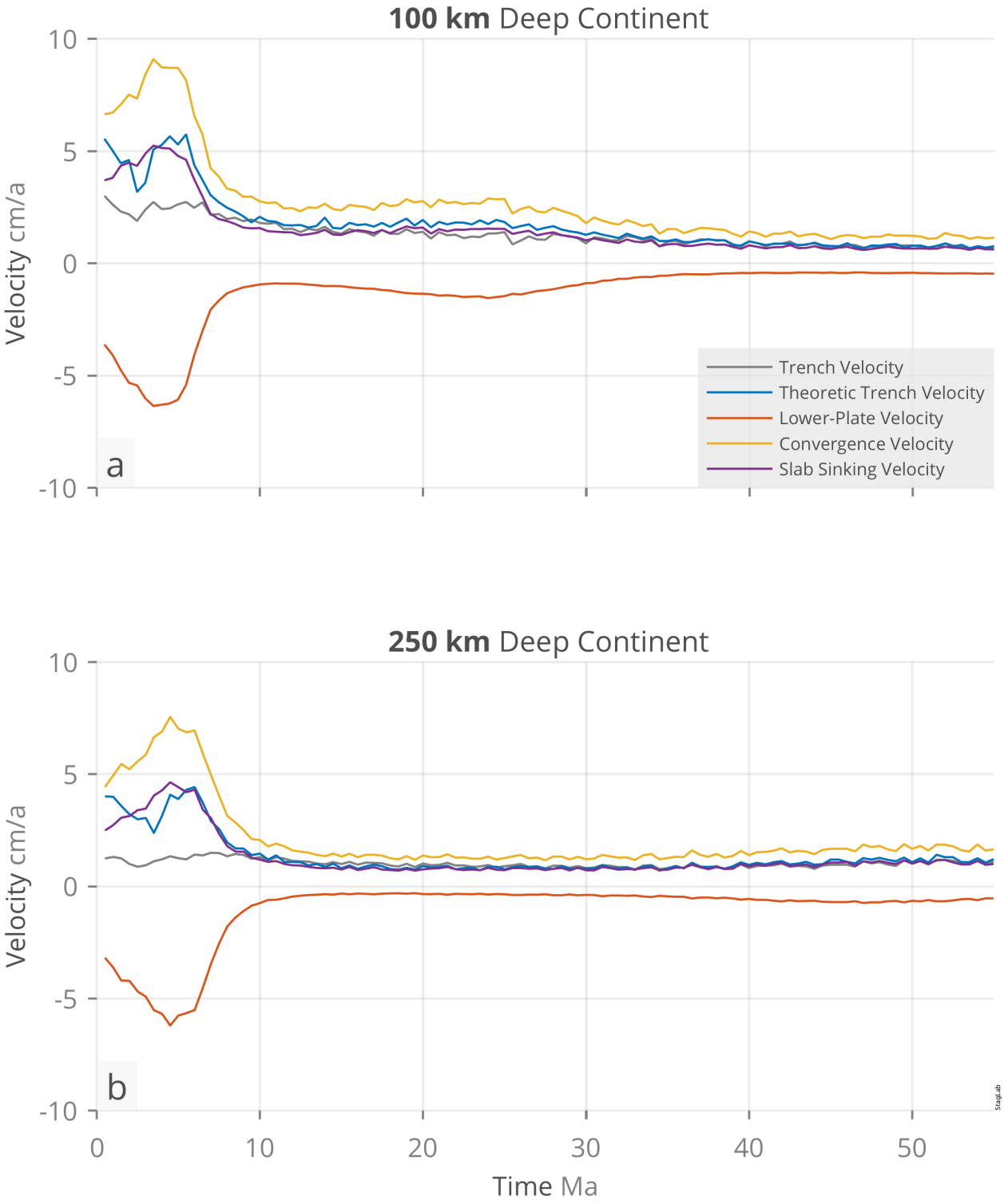

Figure S10: Plate-velocity evolution over time of two experiments of the *Continent* model with (a) a 100 km and (b) a 250 km thick continent. Shown are actual (blue) and theoretic (red) trench velocities, lower-plate velocity (yellow), convergence velocity (purple), and slab sinking velocity (green).

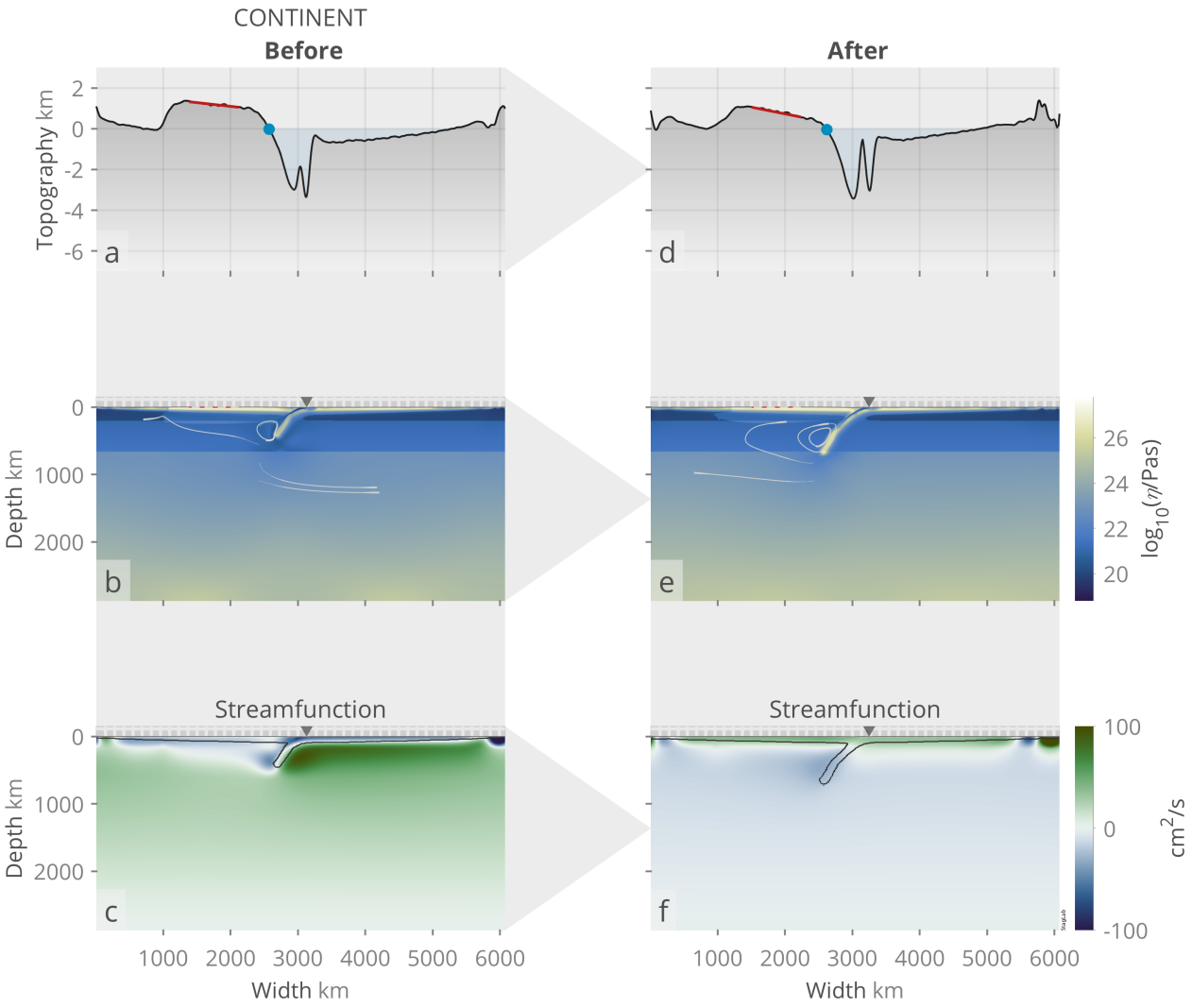

Figure S11: Comparison between (a-c) before and (d-f) after slab-transition zone interaction for the *Continent* model that additionally includes a continental upper plate. Shown are (a,d) surface topography with indicators for upper-plate tilt (red bar) and inundation (blue dot), (b,e) effective viscosity with grey lines indicating flow direction, (c,f) the stream function where blue colours indicate clock-wise direction of the flow and the black contour indicates the position of the plate and slab.

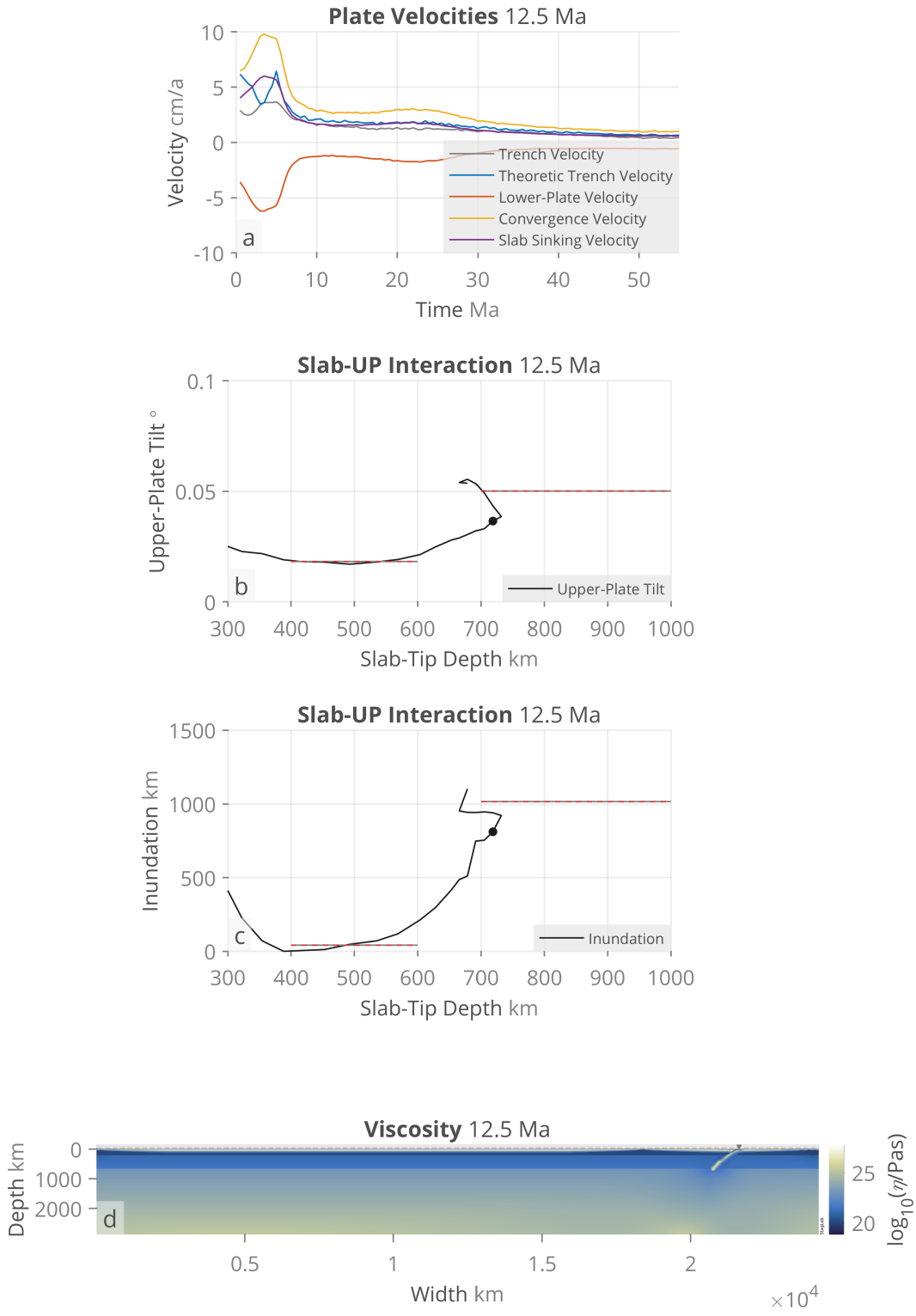

Figure S12: Model domain test: Wider aspect ratio. The *PhaseTransition* model in a wider 8:1 aspect-ratio domain for an experiment employing an initial shallow-slab dip angle of 30°. Shown are (a) temporal evolution of trench and plate velocities, (b) the upper-plate tilt as a function of the slab-tip depth, (c) the upper-plate inundation as a function of the slab-tip depth, and (d) the effective viscosity. Red-grey dashed lines indicate the mean values before and after slab-transition zone interaction and black dots indicate the current time step shown in (d).

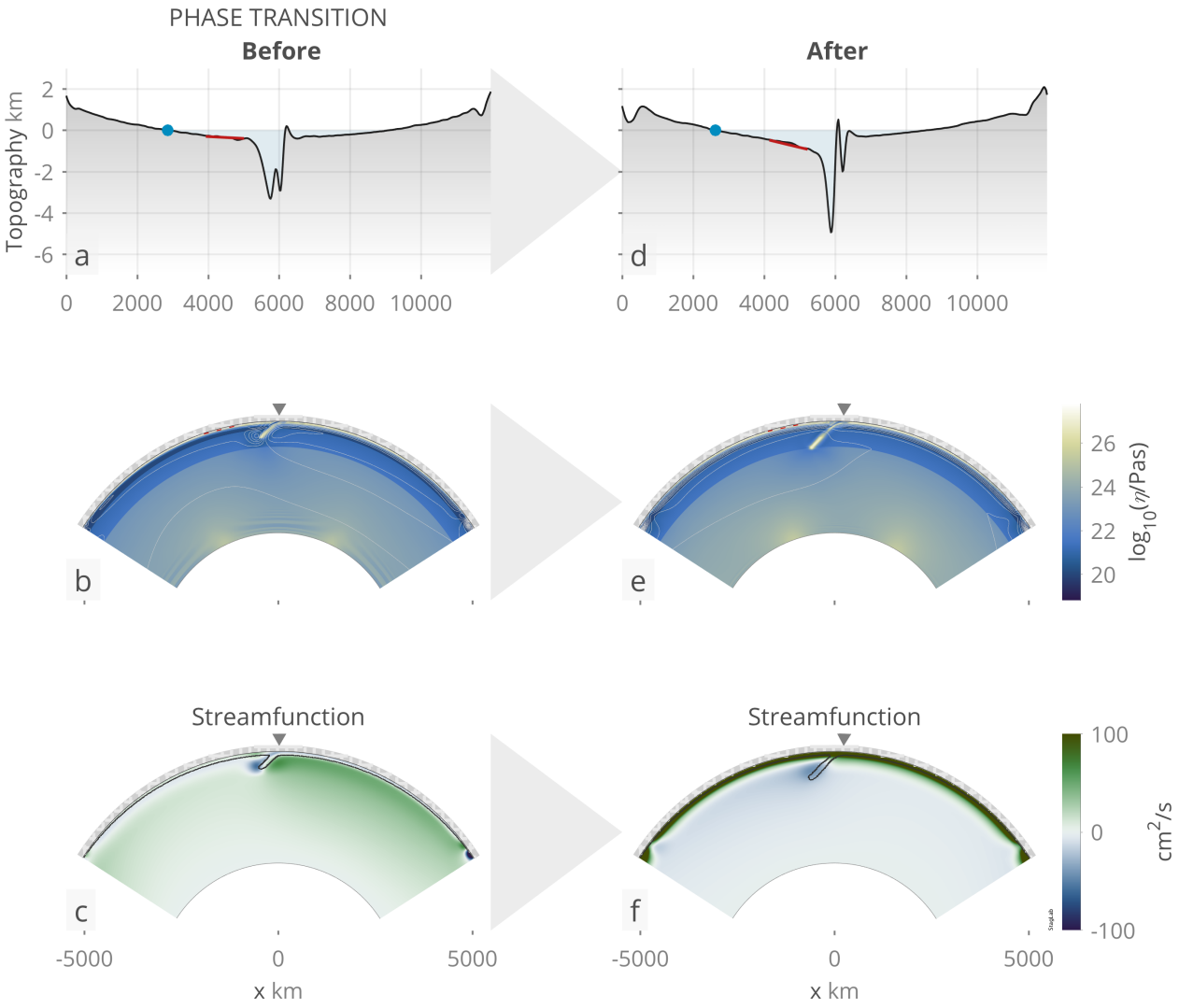

Figure S13: Model domain test: Cylindrical geometry. Comparison between (a-c) before and (d-f) after slab-transition zone interaction for the *PhaseTransition* model in a cylindrical domain that includes an UM-LM phase transition. Shown are (a,d) surface topography with indicators for upper-plate tilt (red bar) and inundation (blue dot), (b,e) effective viscosity with grey lines indicating flow direction, (c,f) the stream function where blue colours indicate clock-wise direction of the flow and the black contour indicates the position of the plate and slab.

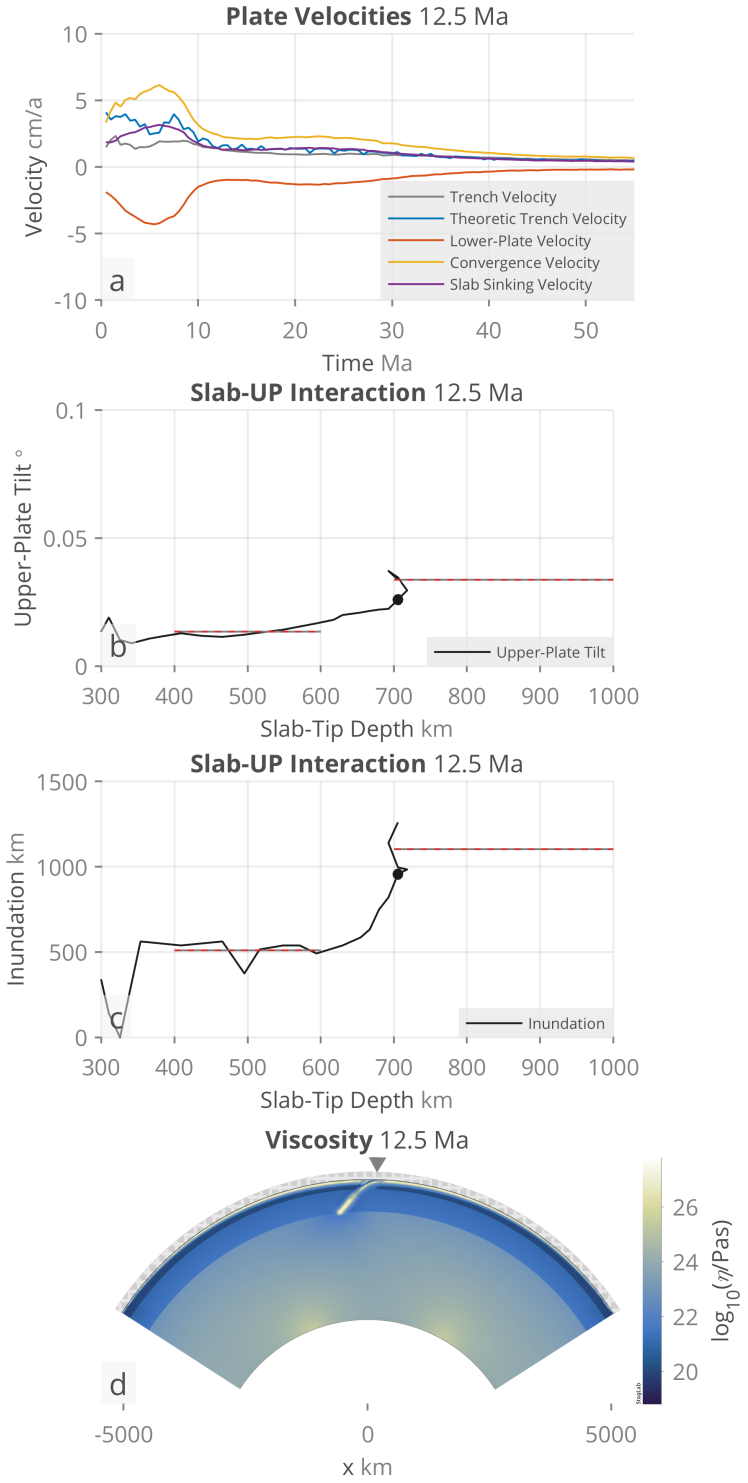

Figure S14: Model domain test: Cylindrical geometry. The *PhaseTransition* model in a cylindrical domain for an experiment employing an initial shallow-slab dip angle of ∼30°. Shown are (a) temporal evolution of trench and plate velocities, (b) the upper-plate tilt as a function of the slab-tip depth, (c) the upper-plate inundation as a function of the slab-tip depth, and (d) the effective viscosity. Red-grey dashed lines indicate the mean values before and after slab-transition zone interaction and black dots indicate the current time step shown in (d).

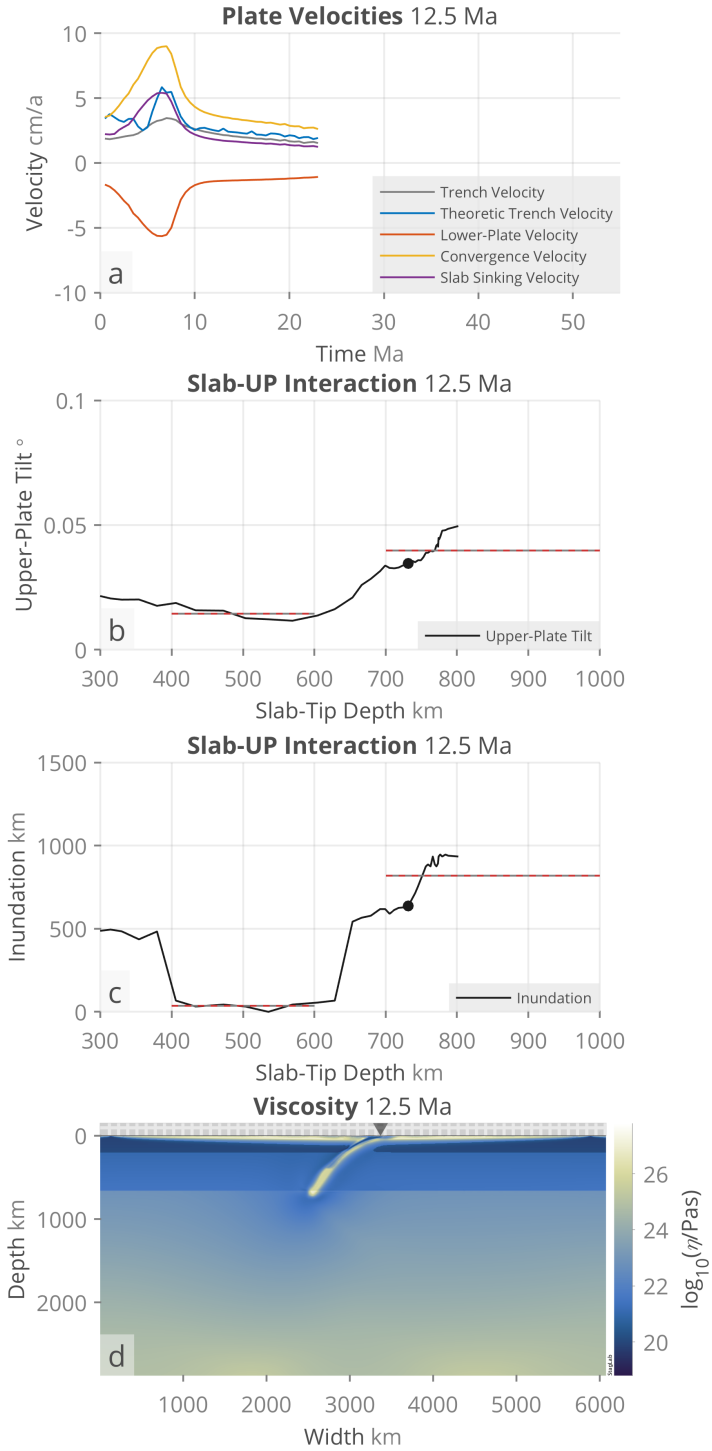

Figure S15: Model domain test: 3-D geometry. The *PhaseTransition* model in a 3-D geometry for an experiment employing an initial shallow-slab dip angle of ∼30° and a lateral, effectively 100-km wide slab gap to allow for toroidal mantle flow. Shown are (a) temporal evolution of trench and plate velocities, (b) the upper-plate tilt as a function of the slab-tip depth, (c) the upper-plate inundation as a function of the slab-tip depth, and (d) the effective viscosity on a vertical slice through the middle of the domain. Red-grey dashed lines indicate the mean values before and after slab-transition zone interaction and black dots indicate the current time step shown in (d).

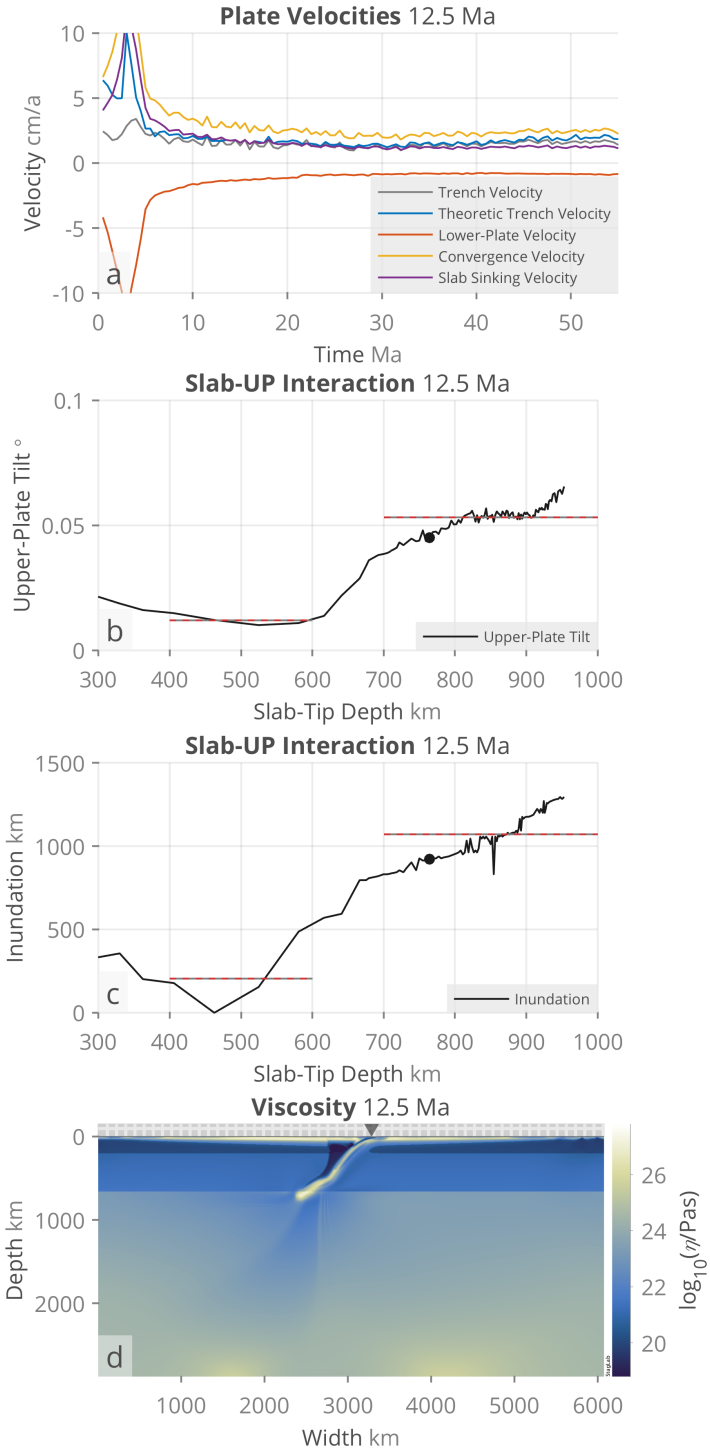

Figure S16: Rheology test: Low-viscosity mantle wedge. The *ViscosityJump* model with the addition of a factor of 100 lower viscosity mantle-wedge for an experiment employing an initial shallow-slab dip angle of ∼30°. Shown are (a) temporal evolution of trench and plate velocities, (b) the upper-plate tilt as a function of the slab-tip depth, (c) the upper-plate inundation as a function of the slab-tip depth, and (d) the effective viscosity. Red-grey dashed lines indicate the mean values before and after slab-transition zone interaction and black dots indicate the current time step shown in (d).